

DETERMINING THE GALACTIC BAR PARAMETERS BASED ON THE HERCULES AND WOLF 630 STELLAR STREAMS

A.T. Bajkova and V.V. Bobylev

Central (Pulkovo) Astronomical Observatory of RAS, 65/1 Pulkovskoye Ch., St. Petersburg, Russia; anisabajkova@rambler.ru

Received: 2016 June 99; accepted: 2016 June 99

Abstract. We have identified the four most significant features in the UV velocity distribution of solar neighborhood stars: H1, H2 and W1, W2 in the Hercules and Wolf 630 streams respectively. We have put the task of determining number of characteristics of the central Galactic bar independently from each of the identified features by assuming that the Hercules and Wolf 630 streams have a bar-induced dynamical nature. The problem has been solved by constructing 2 : 1 resonant orbits in the rotating bar frame for each star in these streams. Analysis of the resonant orbits found has shown that the bar pattern speed Ω_b lies within the range 45–52 km s⁻¹ kpc⁻¹ with a mean of 48.1 ± 1.0 km s⁻¹ kpc⁻¹, while the bar angle θ_b is within the range 35° – 65° with a mean of $50 \pm 4^\circ$. The results obtained are consistent with the view that the Hercules and Wolf 630 streams could be formed by a single mechanism associated with the fact that a long-term influence of the Galactic bar led to a characteristic bimodal splitting of the UV velocity plane.

Key words: Kinematics – Stellar Streams – Hercules Stream – Wolf 630 Stream – Galactic Bar – Galaxy (Milky Way)

1. INTRODUCTION

Analysis of the velocity field of solar-neighborhood stars using Hipparcos (1997) data (Chereul et al. 1998; Dehnen 1998; Asiain et al. 1999; Skuljan et al. 1999) and based on the most recent data (Famaey et al. 2005; Bobylev & Bajkova 2007; Antoja et al. 2008; Bobylev et al. 2010) has revealed a well-developed fine structure. Various nonaxisymmetric Galactic potential models, in particular, the spiral pattern and the Galactic bar, are considered to explain several structures to which quite old stars belong.

As simulations showed, the existence of the Hercules stream can be explained by the fact that its stars have resonant orbits induced by the Galactic bar (Dehnen 1999, 2000; Fux 2001; Chakrabarty 2007; Gardner & Flinn 2010). A detailed analysis of the kinematics of nearby F and G dwarfs using high-resolution spectra (Bensby et al. 2007) showed the stars in the stream to have a wide range of stellar ages, metallicities, and elemental abundances, and this led to the conclusion that the dynamical effect of the Galactic bar is the most acceptable explanation for the existence of the Hercules stream.

In addition to the Hercules stream, there are also other features on the UV

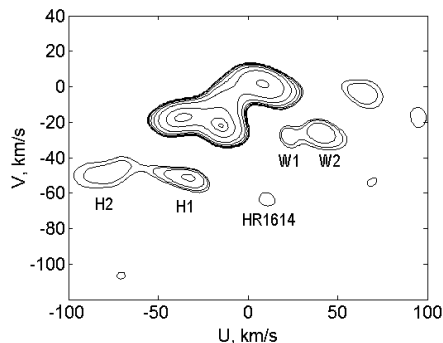


Figure 1: Wavelet map of UV velocities constructed using ~ 17000 single stars from Hipparcos (1997) with relative parallax errors of no more than 10%.

velocity plane, in particular, the Wolf 630 stream (Bobylev et al. 2010), with some of the authors designating this place as the α Ceti stream (Francis & Anderson 2009). The interest is that there are orbits both elongated along the bar major axis and oriented perpendicularly to it in the bar reference frame. At present, there is reason to believe that the Sun is near the point of intersection of such orbits (Fig. 1 in Dehnen 2000). In this case, the bimodality of the UV velocity distribution can be explained by the fact that there are representatives of these two orbit families in the solar neighborhood. According to Dehnen (2000), the detailed form of the velocity distribution depends strongly on the position of the Outer Lindblad Resonance (OLR). In particular, there will be no bimodality if the OLR is farther from the Galactic center than the solar cycle ($R_{OLR}/R_0 > 1.05$, Fig. 4 in Dehnen (2000)). According to the coordinates on the UV velocity plane, the Hercules stream is a representative of the family of orbits oriented perpendicularly to the bar major axis, while the representatives of the family of orbits elongated along the bar major axis are located in the region on the UV velocity plane where the Wolf 630 stream is observed.

The goal of this paper is to estimate such characteristics of the bar as its pattern speed Ω_b and orientation θ_b under the assumption that the Hercules and Wolf 630 streams could be formed by a single mechanism associated with the influence of the Galactic bar. We solve the problem by constructing 2 : 1 resonant orbits in the rotating bar frame. The characteristics of each of the streams are determined independently, i.e., we do not assume them to be of common origin in advance. This work differs from the one published recently (Bobylev & Bajkova 2016), in which for stellar orbit construction we used equations of motion in a coordinate system centered on the Sun and rotating around Galactic center with a constant angular velocity (Fernández et al. 2008, Asiain et al. 1999). In this paper we use more exact equations of motion in Galactic rotating frame based on effective potential $\Phi_{eff}(x, y, z)$ (Jung & Zotos 2016). As a result we have obtained new, slightly different, estimates for the Galactic bar parameters.

2. THE UV VELOCITY DISTRIBUTION OF THE STREAMS

The wavelet map of the UV velocity distribution for single stars with reliable

distance estimates from Bobylev et al. (2010) is presented in Fig. 1. The map was constructed using ~ 17000 stars from the Hipparcos catalogue (1997). We took their proper motions and parallaxes from a revised version of this catalogue (van Leeuwen 2007) and their radial velocities from the OSACA catalogue of radial velocities (Bobylev et al. 2006) and the Pulkovo compilation of radial velocities (PCRv) (Gontcharov 2006). For all these stars, the relative error in the parallax does not exceed 10%.

The contour lines in Fig. 1 are given on a logarithmic scale: 1, 2, 4, 8, ..., 90%, and 99%. The velocities are given relative to the Sun. This figure indicates the W1 and W2 features for the Wolf 630 stream and the H1 and H2 features for the Hercules stream with the following coordinates of their centers: W1 (U, V) = (21, -26) km s⁻¹, W2 (U, V) = (40, -24) km s⁻¹, H1 (U, V) = (-37, -50) km s⁻¹, H2 (U, V) = (-78, -49) km s⁻¹. According to this map, we selected the specific stars belonging to these features based on the probabilistic method. The number of probable candidates in each stream was the following: 250, 271, 401, and 218 stars in W1, W2, H1, and H2, respectively.

When constructing the Galactic orbits to determine the stellar velocities relative to the local standard of rest (LSR), we use the peculiar solar velocity components relative to the LSR with their values from Schönrich et al. (2010), ($U_{\odot}, V_{\odot}, W_{\odot}$) = (11.1, 12.2, 7.3) \pm (0.7, 0.5, 0.4) km s⁻¹.

3. METHOD

3.1. Orbit construction

The Galactic bar follows a clockwise rotation around the z -axis at a constant angular velocity Ω_b . The potential in the rotating frame of reference (known as the effective potential) is (Jung & Zotos 2016)

$$\Phi_{eff}(x, y, z) = \Phi_t(x, y, z) - \frac{1}{2}\Omega_b^2(x^2 + y^2), \quad (1)$$

where $\Phi_t(x, y, z)$ is the total Galactic potential, the coordinate system (x, y, z) is centered on the Galactic center, with the x axis being directed to the Galactic center, the y axis pointing in the direction of Galactic rotation, and the z axis being directed toward the north Galactic pole.

The Hamiltonian which governs the motion of a test particle with a unit mass in our rotating galaxy model is

$$H = \frac{1}{2}(p_x^2 + p_y^2 + p_z^2) + \Phi_t(x, y, z) - \Omega_b L_z = E, \quad (2)$$

where p_x , p_y and p_z are the canonical momenta per unit mass, conjugate to x , y and z respectively, E is the numerical value of the Jacobi integral, which is conserved, while $L_z = xp_y - yp_x$.

The corresponding equations of motion are

$$\begin{aligned}
 \dot{x} &= p_x + \Omega_b y, \\
 \dot{y} &= p_y - \Omega_b x, \\
 \dot{z} &= p_z, \\
 \dot{p}_x &= -\partial\Phi_t/\partial x + \Omega_b p_y, \\
 \dot{p}_y &= -\partial\Phi_t/\partial y - \Omega_b p_x, \\
 \dot{p}_z &= -\partial\Phi_t/\partial z,
 \end{aligned} \tag{3}$$

where the dot indicates the derivative with respect to the time. When the Galactic potential Φ_t is known, the system of equations (3) can be solved numerically. We used a fourth-order RungeKutta integrator.

The Galactic potential $\Phi_t(x, y, z)$, considered here, consists of an axisymmetric component and a bar potential:

$$\Phi = \Phi_o + \Phi_b. \tag{4}$$

In turn, the axisymmetric component can be represented as the sum of three components — central (bulge), disk, and halo ones:

$$\Phi_o = \Phi_C + \Phi_D + \Phi_H. \tag{5}$$

We used the model of Allen & Santillán (1991). The central component of the Galactic potential is represented as

$$\Phi_C = -\frac{M_C}{(x^2 + y^2 + z^2 + b_C^2)^{1/2}}. \tag{6}$$

where M_C is the mass, b_C is the scale length, and $r^2 = x^2 + y^2$,

The disk component is

$$\Phi_D = -\frac{M_D}{\{x^2 + y^2 + [a_D + (z^2 + b_D^2)^{1/2}]^2\}^{1/2}}, \tag{7}$$

where M_D is the mass, a_D and b_D are the scale lengths.

The halo component is

$$\Phi_H = -\frac{M(R)}{R} - \int_R^{100} \frac{1}{R'} \frac{dM(R')}{dR'} dR', \tag{8}$$

where

$$M(R) = \frac{M_H (R/a_H)^{2.02}}{1 + (R/a_H)^{1.02}}.$$

Here, M_H is the mass, a_H is the scale length, and $R^2 = x^2 + y^2 + z^2$.

The triaxial ellipsoid model (Palouš et al. 1993) was chosen as the potential due to the central bar:

$$\Phi_b = \frac{M_b}{(q_b^2 + x^2 + [y a_b/b_b]^2 + [z a_b/c_b]^2)^{1/2}}, \tag{9}$$

where $x = R \cos \vartheta$, $y = R \sin \vartheta$, a_b, b_b, c_b are the three bar semiaxes, q_b is the bar length; $\vartheta = \theta - \Omega_b t - \theta_b$, $tg(\theta) = y/x$; Ω_b is the bar pattern speed, t is the integration time, θ_b is the bar angle relative to the Galactic x and y axes.

The bar is introduced slowly. The total mass in the bar M_b grows with the time

$$M_b(t) = e^{-t_0/t} M_{b,final},$$

where t is the time, $t_0 = 0.5$ Gyr.

If R is measured in kpc, M_C, M_D, M_H, M_b are in units of the Galactic mass (M_G) equal to $2.325 \times 10^7 M_\odot$, then the gravitational constant $G = 1$ and $100 \text{ km}^2 \text{ s}^{-2}$ is the unit of measurement of the potential Φ_t and its individual components (6)–(9). The parameters of the model potential from Allen and Santillán (1991) and the bar potential are: $M_C = 606 M_G$, $M_D = 3690 M_G$, $M_H = 4615 M_G$, $M_b = 43.1 M_G$, $b_C = 0.3873$ kpc, $a_D = 5.3178$ kpc, $b_D = 0.25$ kpc, $a_H = 12$ kpc, $q_b = 5$ kpc, $a_b/b_b = 1/0.42$, $a_b/c_b = 1/0.33$.

In the case of integration by the Runge–Kutta method, it should be kept in mind that $t = 0.001/1.023$ corresponds to one million years at the distance and mass measurements adopted above. The orbit integration time was chosen to be 2.2 Gyr, given that the characteristic lifetime of the bar (from the beginning of its formation to its destruction) is typically 2–4 Gyr.

3.2. Searching for Periodic Orbits

This section is devoted to searching for resonant periodic orbits in an axisymmetric potential in a rotating frame lying in the Galactic plane centered at the Galactic center.

In this paper, as the rotating frame we consider the bar whose pattern speed and orientation we attempt to estimate by constructing the resonant periodic orbits of stars from the Hercules and Wolf 630 streams in the bar frame. This requires finding the periodic orbits that satisfy the (2 : 1) resonance (Fux 2001). The condition for a resonance in the stellar disk plane is the commensurability of two frequencies: the angular velocity Ω and the epicyclic frequency κ :

$$l\kappa = m(\Omega - \Omega_p), \quad (10)$$

with integers $m \geq 0$ and l . In the rotating frame, the m/l resonant orbit is closed after m radial oscillations and $|l|$ orbital periods. Note that condition (10) coincides with the condition for Lindblad resonances only at $l = \pm 1$. The outside corotation, $l < 0$, is negative, and we can talk about the outer $m/|l|$ resonances. In this paper, we discuss only the outer resonances. Fig. 4 from Fux (2001) presents such orbits at $|l| = 1$. If $m = 2$ and $l = -1$, corresponding to (2 : 1) resonant orbits, then it follows from Eq. (10) that

$$\Omega_p = \Omega + \kappa/2. \quad (11)$$

The ideology of the proposed method is that we seek for the bar pattern speed Ω_b (it is different for different stars) at which the orbit becomes resonant and, hence, periodic (in the case of an axisymmetric potential) and quasi-periodic (in the case of a nonaxisymmetric potential, for example, when the bar is included, see below). We propose the following numerical algorithm seeking for such a pattern speed Ω_b lying within the range $[\Omega_1, \Omega_2]$ predetermined empirically:

(1) For a given frequency range, we specify a grid of discrete frequencies $\Omega_1 + m\Delta\Omega$, $m = 0, \dots, M$, where $\Delta\Omega = (\Omega_2 - \Omega_1)/M$, M is an integer large enough to obtain the required dense grid of frequencies. Experience shows that an acceptable accuracy of the algorithm is achieved at $\Delta\Omega = 0.01 \text{ km s}^{-1} \text{ kpc}^{-1}$.

(2) We integrate the stellar orbit equations (3) for a sufficiently long time (several billion years or tens of revolutions around the Galactic center) for each value of $\Omega_b = \Omega_1 + m\Delta\Omega$, $m = 0, \dots, M$ specified above.

(3) We superimpose a discrete grid on the (xy) plane with the same step $\Delta x = \Delta y = \Delta$ in the x and y directions that is chosen empirically to be small enough to provide the required orbit reproduction accuracy. The product $\Delta \times N$, where N is the maximum number of cells in both x and y directions, gives the linear size of the (xy) map.

(4) On the discrete $N \times N$ (xy) plane, we assign “1” to the coordinates of the cell through which the orbit passes and “0” to all the remaining discrete coordinates. If the orbit crosses a given cell several times, then we anyway assign “1” to the corresponding point on the plane only once.

(5) For all maps, we count the number of “1”. The map with the smallest number of “1” corresponds to the orbit with a resonance frequency $\Omega_b = \Omega_1 + i\Delta\Omega$, where i is the map number.

Note that this algorithm slightly differs from the one proposed by Bobylev & Bajkova (2016) because of another form of equations of motion.

Stable periodic orbits give a filling in the form of a trajectory whose shape does not change with increasing number of revolutions around the Galactic center. If several stable periodic orbits fall within a given frequency range, then the algorithm chooses the orbit with the smallest filling to which the orbit with the smallest multiplicity of resonance frequencies corresponds. If the orbit is not stable, then it progressively densely fills a certain space on the (xy) coordinate plane with increasing integration time or number of revolutions around the Galactic center.

We also studied influence of the bar to the resonance orbits. Naturally, introducing the bar leads in general to non-periodic (quasi-periodic) orbits acquiring the property of stochasticity. But, it turned out that when the bar was included, the resonance frequencies changed by a negligibly small value, while the shape and orientation of orbits in the bar frame practically did not change. Thus, we showed that to solve our problem of determining the bar pattern speed and orientation, it would suffice to study the periodic orbits obtained in the axisymmetric potential. This is important, because the bar potential is not known with certainty; there are a multitude of its models in the literature. We only know that its gravitational contribution to the total Galactic potential is small.

The bar orientation in the Galactic (xy) plane can be determined from the orientation of resonant orbits in the bar rotating frame. Indeed, while in the axisymmetric case the orientation of the resonant orbits is arbitrary, the virtual introduction of a bar will retain only those orbits which are reflection symmetric with respect to at least one of the bar principal axes (Fux 2001).

4. RESULTS AND DISCUSSION

Using the above-described method of searching for periodic orbits in an axisymmetric potential for each star of the identified H1, H2, W1, and W2 features, we found the resonance frequencies $\Omega_{2:1}$. The interval of integration was 2.2 Gyr.

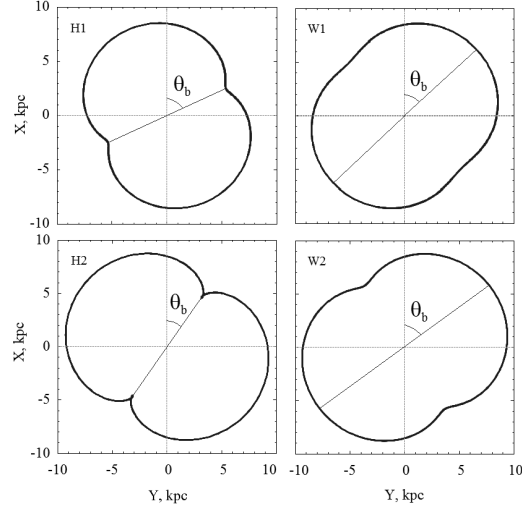


Figure 2: Resonant periodic orbits in the bar rotating frame constructed from averaged data on stars of H1, H2 and W1, W2 streams in axisymmetric Galactic potential. The Galactic center lies at the coordinate origin; the Sun's coordinates are $(x, y) = (8.5, 0)$ kpc; θ_b is the bar angle counted from the direction to the Sun.

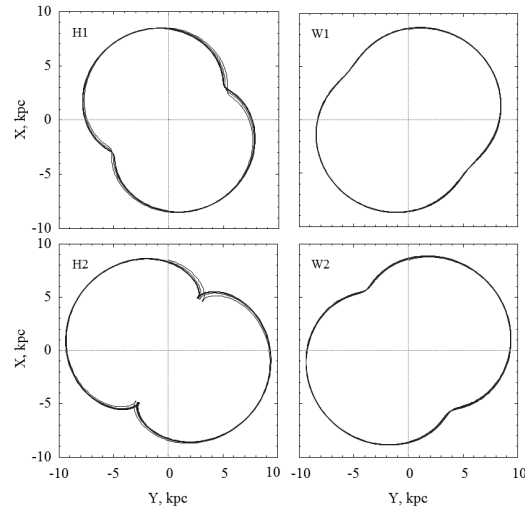


Figure 3: Resonant orbits in the bar rotating frame constructed from averaged data on stars of H1, H2 and W1, W2 streams in nonaxisymmetric Galactic potential (with the bar).

Table 1: Parameters found from the H1, H2 and W1, W2 features

Feature	Ω_b , km s ⁻¹ kpc ⁻¹	θ_b , deg
H_1	51.4 ± 0.8	65 ± 4
H_2	49.1 ± 1.4	35 ± 5
W_1	46.5 ± 0.8	45 ± 3
W_2	45.3 ± 1.0	55 ± 4
Mean	48.1 ± 1.0	50 ± 4

Fig. 2 presents the resonant periodic orbits in the bar rotating frame constructed from averaged data on coordinates and velocities of stars included in H1, H2 and W1, W2 streams using axisymmetric Galactic potential. Fig. 3 shows the similar resonant orbits constructed using nonaxisymmetric Galactic potential which includes the potential of the bar. When the bar was included, the resonance frequencies changed by a very small value (on average, 0.4%), while the shape and orientation of orbits in the bar frame practically did not change. Therefore we determined parameters of the bar from the periodic orbits (Fig.2).

As can be seen from Fig. 2, the orbits corresponding to H1 and H2 streams are elongated perpendicularly to the bar major axis, while the W1 and W2 orbits are elongated along the bar, the bar angle θ_b lies within the range $35^\circ - 65^\circ$. In accordance with the central limit theorem, we assume that the deviations of the resonance frequencies and the orbital inclinations of stars from the samples considered obey a normal law. Both Ω_b and θ_b for each sample were calculated as the mean values of the individual parameters of stars from the samples; the errors in Ω_b and θ_b were calculated as the root-mean-square deviation from the mean. The results obtained are presented in Table 1.

So, the resonant periodic orbits we found show that the bar pattern speed Ω_b lies within the range $45-52$ km s⁻¹ kpc⁻¹ with a mean of 48.1 ± 1.0 km s⁻¹ kpc⁻¹, while the bar angle θ_b is within the range $35^\circ - 65^\circ$ with a mean of $50 \pm 4^\circ$. These parameters differ a little from the previously obtained (compare with Table 2 from Bobylev & Bajkova (2016)).

The results obtained are consistent with the view that the Hercules and Wolf630 streams could be formed by a single mechanism associated with the splitting of the UV velocity plane under the influence of the Galactic bar. Our results are in agreement with the simulations of Dehnen (1999) for $R_{OLR} \approx 0.9R_0$, while in our case, as shown in Bobylev & Bajkova (2016), $R_{OLR} = 0.93R_0$

5. CONCLUSIONS

We analyzed the four most significant features in the UV velocity distribution of solar-neighborhood stars: H1, H2 from the Hercules stream and W1, W2 from the Wolf630 stream with the (U, V) coordinates of their centers $(-37, -50)$, $(-78, -49)$, $(21, -26)$, and $(40, -24)$ km s⁻¹, respectively. Based on the assumption that the Hercules and Wolf630 streams were induced by the central Galactic bar, we formulated the problem of determining the bar characteristics independently from each of the identified features.

To construct the Galactic orbits of the individual stars forming these streams,

we used the Galactic potential model of Allen & Santillán (1991) and the equations of motion in Galactic rotating frame based on effective potential $\Phi_{eff}(x, y, z)$ (Jung & Zotos 2016). From the set of constructed orbits, we selected only the stable orbits in resonance with the bar. Analysis of the resonant orbits found showed that the bar pattern speed Ω_b lies within the range 45–52 km s⁻¹ kpc⁻¹ with a mean of 48.1 ± 1.0 km s⁻¹ kpc⁻¹, while the bar angle θ_b is within the range 35° – 65° with a mean of $50 \pm 4^\circ$. These estimates differ slightly from the previously obtained (Bobylev & Bajkova 2016).

The results obtained are consistent with the view that the Hercules and Wolf630 streams could be formed by a single mechanism associated with the fact that a long-term influence of the Galactic bar led to a characteristic bimodal splitting of the *UV* velocity plane.

ACKNOWLEDGMENTS. This study was supported by the “Transient and explosive processes in Astrophysics” Program of the Presidium of Russian Academy of Sciences (P-7).

REFERENCES

- Allen C. and Santillán A., 1991, *Rev. Mex. Astron. Astrof.*, 22, 255
 Antoja T., Figueras F., Fernández D., et al., 2008, *A&A*, 490, 135
 Asiain R., Figueras F., Torra J., et al., 1999, *A&A*, 341, 427
 Bensby T., Oey M. S., Feltzing S., et al., 2007, *ApJ*, 655, L89
 Bobylev V. V., Gontcharov G. A., Bajkova A. T., 2006, *Astron. Rep.*, 50, 733
 Bobylev V. V., Bajkova A. T., 2007, *Astron. Rep.*, 51, 372
 Bobylev V. V., Bajkova A. T., Mylläri A. A., 2010, *Astron. Lett.*, 36, 27
 Bobylev V. V., Bajkova A. T., 2016, *Astron. Lett.*, 42, 228
 Chakrabarty D., 2007, *A&A*, 467, 145
 Chereul E., Crézé M., Bienaymé O., 1998, *A&A*, 340, 384
 Dehnen W., 1998, *AJ*, 115, 2384
 Dehnen W., 1999, *ApJ*, 524, L35
 Dehnen W., 2000, *AJ*, 119, 800
 Famaey B., Jorissen A., Luri X., et al., 2005, *A&A*, 430, 165
 Fernández D., Figueras F., Torra J., 2008, *A&A*, 480, 735
 Francis C., Anderson E., 2009, *New Astron.*, 14, 615
 Fux R., 2001, *A&A*, 373, 511
 Gardner E., Flinn C., 2010, *MNRAS*, 405, 545
 Gontcharov G. A., 2006, *Astron. Lett.* 32, 795
 The Hipparcos and Tycho Catalogues, 1997, ESA SP-1200
 Jung C., Zotos E. E., 2016, *MNRAS*, 457, 2583
 van Leeuwen F., 2007, *A&A*, 474, 653
 Palouš J., Jungwiert B., Kopecký J., 1993, *A&A*, 274, 189
 Schönrich R., Binney J., Dehnen W., 2010, *MNRAS*, 403, 1829
 Skuljan J., Hearnshaw J. B., Cottrell P. L., 1999, *MNRAS*, 308, 731